Nuclear Instruments and Methods in Physics Research B 269 (2011) 2610–2613

Contents lists available at ScienceDirect

Nuclear Instruments and Methods in Physics Research B

journal homepage: www.elsevier.com/locate/nimb

EXAFS and SR-XRD study on Mn occupations in $Zn_{1-x}Mn_xO$ diluted magnetic semiconductors

M. Li [a,b], B. Zhang [a,b,*], J.Z. Wang [a,b], L.Q. Shi [a,b], H.S. Cheng [a,b], Y.Z. Wang [a,b], H.Y. Lv [a,b], T.Y. Yang [c], W. Wen [c], F.C. Hu [d]

[a] Applied Ion Beam Physics Laboratory (Key Laboratory of the Ministry of Education), Institute of Modern Physics, Fudan University, Shanghai 200433, PR China
[b] Department of Nuclear Science and Technology, Fudan University, Shanghai 200433, PR China
[c] Shanghai Institute of Applied Physics, Chinese Academy of Sciences, Shanghai 201204, PR China
[d] National Synchrotron Radiation Laboratory, University of Science and Technology of China, Hefei 230029, PR China

ARTICLE INFO

Article history:
Received 15 January 2011
Received in revised form 17 July 2011
Available online 26 July 2011

Keywords:
EXAFS
SR-XRD
PIXE
Mn occupations
ZnO DMS

ABSTRACT

Mn-doped ZnO films were prepared by radio frequency (RF) magnetron sputtering on sapphire substrate. Mn content was determined by proton induced X-ray emission (PIXE). Only Mn, no other magnetic impurities such as Fe, Co and Ni were observed. Also, no precipitates such as MnO, Mn_3O_4 and other secondary phases or Mn clusters, were found by SR-XRD, even in Mn-doped content up to 11 at.%. EXAFS analyses showed that Mn atoms were incorporated into ZnO crystal lattice by occupying the sites of zinc atoms.

1. Introduction

ZnO-based diluted magnetic semiconductor (DMS) is a kind of the preferred material for spintronics device. Since Ditel et al. [1] theoretically predicted that ZnO doped with 5 at.% Mn might exhibit room temperature ferromagnetism, a number of studies have been made to develop this promising (Zn, Mn)O DMS material. Until now, there have been many reports on room temperature ferromagnetism in this system [2–7]. However, it is still a controversial issue whether the observed ferromagnetism is intrinsic or comes from the precipitates (e.g., clusters and/or a secondary phase) [8–10]. Generally, Mn impurity atoms can occupy not only the cation sites but also the interstitial sites during the growth of material. Especially, the precipitates such as Mn compounds and/or clusters can form at high Mn doped content. Their amount in ZnO substrate is usually too small to be detected by conventional techniques. Therefore, to understand the ferromagnetic origin, it is essential to use the detective method of high sensitivity such as extended X-ray absorption fine structure (EXAFS) and synchrotron radiation X-ray diffraction (SR-XRD).

In this paper, we adopt these two techniques to study on Mn occupation site in Mn doped ZnO films grown by radio frequency (RF) magnetron sputtering. It has shown that in our samples, any precipitates such as MnO, Mn_3O_4 and other secondary phases or Mn clusters, are not found, even in an 11 at.% Mn-doped content. Mn atoms are incorporated into ZnO crystal lattice through the substitution on Zn sites.

2. Experiment

Mn-doped ZnO films were deposited on (0 0 0 1) sapphire substrates (99.999%) by radio frequency (RF) magnetron sputtering, with a composite target of ZnO (99.99%) and Mn (99.99%). According to the area ratio of ZnO and Mn, the Mn-doped content was adjusted. High purity Ar (99.999%) was introduced into the sputtering chamber after the base pressure fell below 6.0×10^{-4} Pa. The flow rate of Ar was kept at 20 SCCM (SCCM denotes cubic centimeter per minute at STP (standard temperature and pressure)). The working pressure was fixed at 0.5 Pa and the sputtering power was 90 W. The substrate temperature was kept at 500 °C. Prior to deposition, a pre-sputtering cleaning was performed for about 20 min to eliminate possible contaminants from the target surface.

The external-beam proton induced X-ray emission (PIXE) [11,12] was employed to determine Mn-doped content at the NEC 9SDH-2 3 MV pelletron tandem accelerator of Fudan University. Samples were placed at 10 mm outside the beam exit window

* Corresponding author at: Applied Ion Beam Physics Laboratory (Key Laboratory of the Ministry of Education), Institute of Modern Physics, Fudan University, Shanghai 200433, PR China. Tel.: +86 2155665192; fax: +86 2165642787.
E-mail address: binzhang@fudan.edu.cn (B. Zhang).

0168-583X/$ - see front matter © 2011 Elsevier B.V. All rights reserved.
doi:10.1016/j.nimb.2011.07.094

(7.5 μm Kapton film). A ORTEC Si(Li) detector (165 eV FWHM at 5.9 keV) placed perpendicular to the beam direction, was used to detect the X-ray emitted from the sample. X-rays traveled through 10–15 mm of air before reaching the detector. A 3.0-MeV collimated proton beam with diameter of 1 mm was used and beam current was 0.1–1.0 nA keeping the dead time less than 5%. The obtained PIXE spectrum was recorded and analyzed with conventional electronic system followed by a multi-channel analyzer. The yields of the characteristic X-ray peaks were obtained after background fitting and subtraction using the program GUPIX-96 [13]. The PIXE system was calibrated by using the X-ray of 5.894 keV emitted from the ^{55}Fe radioactive source and the detector efficiency for the Mn K lines was almost 100%. The reference sample GSD-6, whose element contents have been measured by the inductively coupled plasma method, was used to determine the PIXE experimental parameters (e.g., the solid angle of detector and the distance between the target and detector). The details of the experimental method and the PIXE setup have been described elsewhere [14–16]. X-ray diffraction measurements were performed at beamline BL14B1 of Shanghai Synchrotron Radiation Facility (SSRF) using a wavelength of 0.12398 nm. The Mn K-edge EXAFS spectra were measured at the U7C beamline of National Synchrotron Radiation Laboratory of China.

3. Results and discussion

Fig. 1 is typical PIXE spectra of the samples. The PIXE spectra show only peaks corresponding to Mn, Zn, Ar from air, and Al from Al_2O_3 substrate. It means that only Mn, no other magnetic impurities such as Fe, Co and Ni exist in these films. Using a program GUPIX-96 [13], we obtain 2 ± 0.06, 5 ± 0.10, 7 ± 0.14 and 11 ± 0.20 at.% of Mn-doped content, respectively. The relative error of Mn content is below 3%.

Fig. 2 shows SR-XRD pattern of the samples. Except the (0 0 0 6) peak of Al_2O_3 substrate, the (0 0 0 2) and (0 0 0 4) peaks can be indexed to the wurtzite ZnO structure. Obviously, no trace of secondary phases or clusters (e.g., Mn cluster, MnO and Mn_3O_4) are observed in any of the samples doped with Mn up to 11 at.%.

The EXAFS spectra were measured at the Mn K-edge (6.539 keV) at room temperature in fluorescence mode. Fig. 3(a) and (b) show the Mn K-edge EXAFS $k^3\chi(k)$ functions and their Fourier transform (FT), respectively. The dot lines are from experiment and the color lines are the fitting curves done by using the IFEFFIT 1.2.6 package [17]. For comparison, the $k^3\chi(k)$ and FT curves of the reference

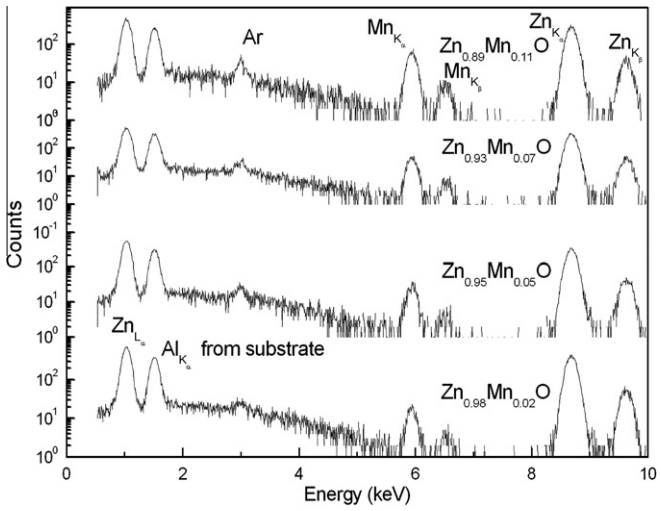

Fig. 1. Typical PIXE spectra of the samples.

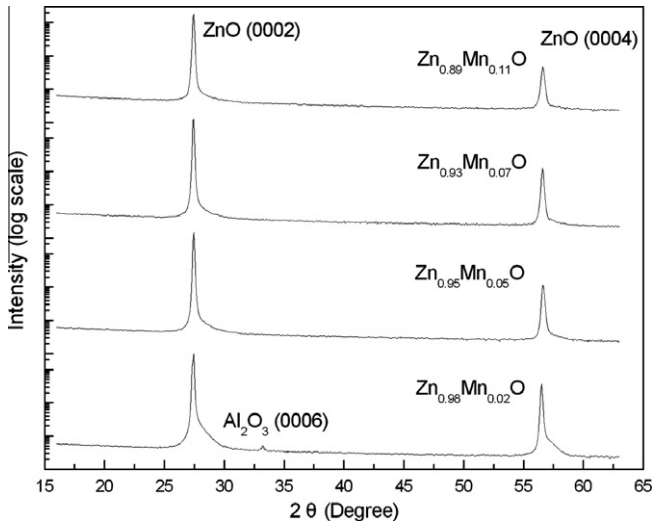

Fig. 2. SR-XRD spectra of the samples.

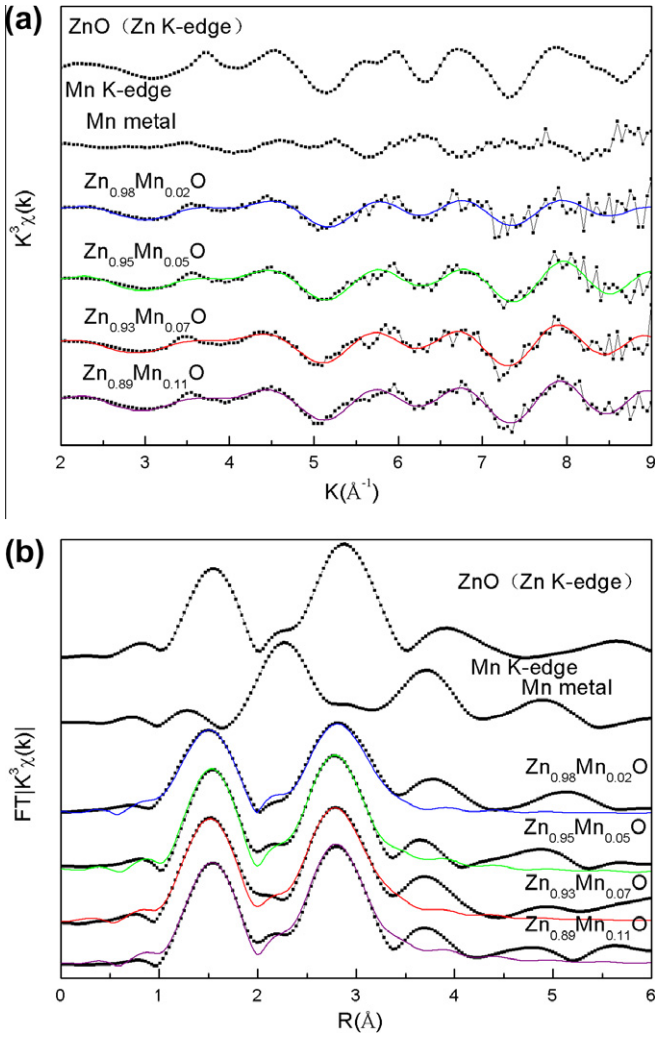

Fig. 3. Mn K-edge EXAFS $k^3\chi(k)$ functions of $Zn_{1-x}Mn_xO$ films (a), and the Fourier transform (FT) of $k^3\chi(k)$ (b).

samples Mn metal and ZnO are also added into Fig. 3(a) and (b). The FT shapes for four samples are different from Mn metal and

same as ZnO. This can exclude the existence of Mn clusters in our samples, which agrees with the SR-XRD results.

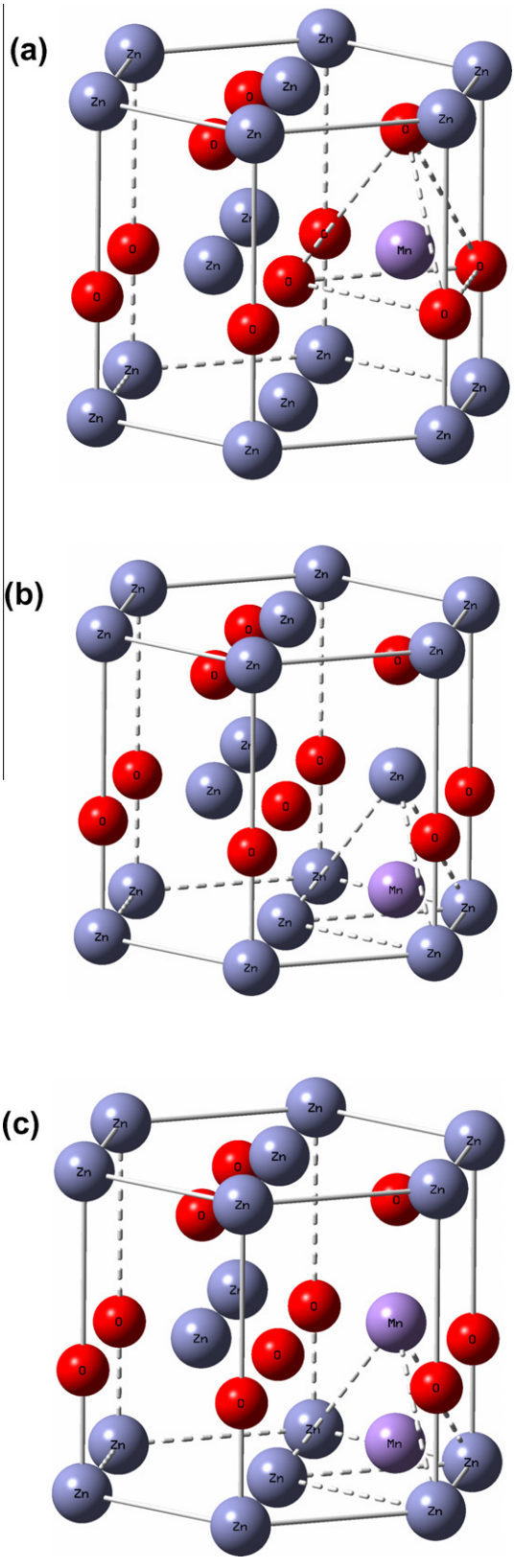

Fig. 4. Model structures of various Mn occupation sites in wurtzite ZnO lattice: (a) substitutional Mn_{Zn}, (b) interstitial Mn_I, and (c) Mn_{Zn}–Mn_I dimmer.

Table 1
Curve-fitting results of all samples.

Sample	Bound type	N	R (Å)	σ^2 (Å^2)
$Zn_{0.98}Mn_{0.02}O$	Mn–O	4	2.01 ± 0.02	0.0081 ± 0.0011
	Mn–Zn	12	3.26 ± 0.03	0.0135 ± 0.0011
$Zn_{0.95}Mn_{0.05}O$	Mn–O	4	2.03 ± 0.02	0.0049 ± 0.0007
	Mn–Zn	12	3.26 ± 0.02	0.0091 ± 0.0007
$Zn_{0.93}Mn_{0.07}O$	Mn–O	4	2.02 ± 0.02	0.0038 ± 0.0010
	Mn–Zn	12	3.29 ± 0.03	0.0092 ± 0.0010
$Zn_{0.89}Mn_{0.11}O$	Mn–O	4	2.03 ± 0.02	0.0047 ± 0.0008
	Mn–Zn	12	3.28 ± 0.02	0.0086 ± 0.0008

N is the coordination number, R the distance between central Mn atoms and coordination atoms, σ^2 the mean square disorder.

In order to investigate further the Mn occupations, we have attempted to model a lot of possible configurations such as the substitutional Mn_{Zn}, the interstitial Mn_I and the Mn_{Zn}–Mn_I dimmer, as shown in Fig. 4. For the interstitial Mn_I model, Mn was placed at the void in wurtzite ZnO structure locating at the center of the Zn tetrahedron. The Mn_{Zn}–Mn_I dimmer was based on the interstitial structure, where one Zn atom of the Mn-containing tetrahedron was substituted by a Mn atom. All EXAFS functions were calculated by FEFF6L [18] with the cluster radius taken as 6 Å. Among these possible models, the experimental spectra can be well fitted only by using the model of the substitutional Mn_{Zn}, as shown in Fig. 3(b). The local structure parameters for our samples obtained from this curve-fitting process are listed in Table 1. From Table 1, the average amount of 4 oxygen atoms surrounding the central Mn atom at a distance of 2.01–2.03 Å as the nearest neighbors, and 12 zinc atoms at 3.26–3.29 Å as the next nearest neighbors are close to that around Zn in ZnO. Xu et al. [19] reported the distances of Mn_{Zn}–O and Mn_{Zn}–Zn were 2 and 3.27 Å, respectively in ZnO-based DMSs. Our results are identical with those of Xu. In the wurtzite ZnO, each Zn atom is surrounded by an average of 4O and 12Zn for the first and second nearest neighbor atoms, respectively at distances of 1.97 and 3.20 Å according to our calculation. The bond lengths of both Mn_{Zn}–O and Mn_{Zn}–Zn in these Mn-doped ZnO films are found to be elongated, which might be ascribed to the larger atomic radius of Mn compared with Zn. This expansion of bond length is also consistent with the results from other investigators [20,21]. Therefore, Mn atoms are incorporated into ZnO crystal lattice by the substitution on Zn sites.

4. Conclusion

Mn-doped ZnO films were prepared by radio frequency (RF) magnetron sputtering on sapphire substrate. Only Mn and no other magnetic impurities such as Fe, Co and Ni were observed. Also, no precipitates such as MnO, Mn_3O_4 and other secondary phases or Mn clusters, were found by SR-XRD, even at an 11 at.% content. Based on EXAFS analyses, Mn atoms were incorporated into ZnO crystal lattice through the substitution of Zn sites.

Acknowledgments

This work is supported by the National Natural Science Foundation of China (Grant Nos. 10775033 and 11075038). We also gratefully acknowledge the supports from Shanghai Leading Academic Discipline Project (Project Number: B107). The authors thank beamline BL14B1 (Shanghai Synchrotron Radiation Facility) in providing the beam time. And also, the authors would like to thank the U7C beamline of National Synchrotron Radiation Laboratory of China for providing the beam time.

References

[1] T. Dietl, H. Ohno, F. Matsukura, J. Cibert, D. Ferrand, Science 287 (2000) 1019.
[2] S.W. Jung, S.J. An, G.C. Yi, C.U. Jung, S.L. Lee, S. Cho, Appl. Phys. Lett. 80 (2002) 4561.
[3] R.K. Zheng, H. Liu, X.X. Zhang, V.A.L. Roy, A.B. Djurisic, Appl. Phys. Lett. 85 (2004) 2589.
[4] V.A.L. Roy, A.B. Djurisic, H. Liu, X.X. Zhang, Y.H. Leung, M.H. Xie, J. Gao, H.F. Liu, C. Surya, Appl. Phys. Lett. 84 (2004) 756.
[5] P. Sharma, A. Gupta, K.V. Rao, F.J. Owens, R. Verma, R. Ahuja, J.M.O. Guillen, B. Johansson, G.A. Gehring, Nat. Mater. 2 (2003) 673.
[6] D. Kundaliya, S. Ogale, S. Lofland, S. Dhar, C. Metting, S. Shinde, Z. Ma, B. Varughese, K. Ramanujachary, L. Salamanca-Riba, T. Venkatesan, Nat. Mater. 3 (2004) 709.
[7] J.M. Baik, J.L. Lee, Adv. Mater. 17 (2005) 2745.
[8] D.P. Norton, M.E. Overberg, S.J. Pearton, K. Pruessner, J.D. Budai, L.A. Boatner, M.F. Chisholm, J.S. Lee, Z.G. Khim, Y.D. Park, R.G. Wilson, Appl. Phys. Lett. 83 (2003) 5488.
[9] R.K. Zheng, H. Liu, X.X. Zhang, V.A.L. Roy, A.B. Djurisic, Appl. Phys. Lett. 85 (2004) 2589.
[10] T.C. Kaspar, T. Droubay, S.M. Heald, M.H. Engelhard, P. Nachimuthu, S.A. Chambers, Phys. Rev. B 77 (2008) 201303.
[11] B. Zhang, Q.H. Li, L.Q. Shi, H.S. Cheng, J.Z. Wang, J. Vac. Sci. Technol. A 26 (2008) 1469.
[12] B. Zhang, L.Q. Shi, C.C. Chen, D.G. Zhao, Nucl. Instr. and Meth. 252 (2006) 225.
[13] J.L. Campbell, T.L. Hopman, J.A. Maxwell, Z. Nejedly, Nucl. Instr. and Meth. 170 (2000) 193.
[14] B. Zhang, B.H. Pan, Z.Q. Zhang, H.S. Cheng, M.H. Gao, F.J. Yang, X.B. Peng, Nucl. Instr. and Meth. 219–220 (2004) 26.
[15] B. Zhang, Q.H. Li, L.Q. Shi, H.S. Cheng, J.Z. Wang, Nucl. Instr. and Meth. 266 (2008) 4891.
[16] B. Zhang, C.C. Chen, C. Yang, J.Z. Wang, L.Q. Shi, H.S. Cheng, D.G. Zhao, Nucl. Instr. and Meth. 268 (2010) 123.
[17] M. Newville, J. Synchrotron Radiat. 8 (2001) 322.
[18] J.J. Rehr, R.C. Albers, Rev. Modern Phys. 72 (2000) 621.
[19] W. Xu, Y.X. Zhou, X.Y. Zhang, D.L. Chen, Y. Xie, T. Liu, W.S. Yan, S.Q. Wei, Solid State Commun. 141 (2007) 374.
[20] H.Y. Xu, Y.C. Liu, C.S. Xu, Y.X. Liu, C.L. Shao, R. Mu, J. Chem. Phys. 124 (2006) 074707.
[21] E. Chikoidze, Y. Dumont, F. Jomard, D. Ballutaud, P. Galtier, O. Gorochov, D. Ferrand, J. Appl. Phys. 97 (2005) 10D327.